Electronic Supplementary Material (ESI) for Chemical Communications

Supporting Information

Polyoxometalate-Based Single-Molecule Magnet with a Mixed-Valent $\{Mn^{IV}_2Mn^{III}_6Mn^{II}_4\}$ Core

Zhi-Ming Zhang,[a] Shuang Yao,[b] Yang-Guang Li,*[a] Hai-Hong Wu,[a] Yong-Hui Wang,[a] Mathieu Rouzières,[c,d] Rodolphe Clérac,*[c,d] Zhong-Min Su,[a] and En-Bo Wang,*[a]

CONTENTS

Section 1 Experimental Section

1. Materials and Methods. All the reagents were commercially purchased and used without further purification. The $K_8[\beta\text{-}SiW_{11}O_{39}]\cdot 14H_2O$ precursor was synthesized according to the literature[S1] and characterized by IR spectrum. Elemental analyses (C and H) were performed on a PerkinElmer 2400 CHN element analyzer; Si, W, Mn, K and Na were analyzed on a PLASMASPEC(I) ICP atomic emission spectrometer. IR spectroscopy was recorded in the range 400-4000 cm^{-1} on an Alpha Centauri FTIR spectrophotometer using KBr pellets. TG analyses were performed on a Perkin–Elmer TGA7 instrument in flowing N_2 with a heating rate of 10 °C•min^{-1}.

2. Synthesis. 1.0 g of $K_8[\beta\text{-}SiW_{11}O_{39}]\cdot 14H_2O$ (0.3 mmol) was dissolved in 30 mL water and $MnCl_2\cdot 4H_2O$ (1.0 g, 5.05 mmol) were added, followed by addition of 2,3-pyrazinedicarboxylic acid (0.10 g, 0.6 mmol) and NaCl solid (0.20 g, 3.4 mmol). Then, the pH value of the mixture was adjusted to 10.2 by slowly adding 2 M K_2CO_3 aqueous solution into the reaction solution. Then, the mixture was stirred at 50 °C for 5 h. After cooling down to the room temperature, a brown residue was filtered. The filtrate was kept undisturbed for slow evaporation. The deep-brown block crystals were isolated in two weeks (Yields: 38% based on W). Anal. Found (%): C, 1.22; H, 1.38; K, 5.69; Na, 4.39; Mn, 12.10; Si, 0.91; W, 40.69; Calcd: C, 1.34; H, 1.27; K, 5.80; Na, 4.26; Mn, 12.22; Si, 1.04; W, 40.87. IR (KBr pellet, cm^{-1}): 1637 (m), 1504 (s), 1316 (s), 1060 (m), 970 (m), 842 (m), 873 (s), 803 (m), 686 (w), 615 (w), 580 (w), 532 (w), 500 (w) and 436 (w).

3. X-ray Crystallography. The crystallographic data was performed on a Rigaku R-AXIS RAPID IP diffractometer. The data were collected at 293 K, and graphite-monochromated Mo-Kα radiation (λ = 0.71073 Å). The structures were solved by the direct method and refined by the

Full-matrix least squares on F^2 using the SHELXL-97 software.[S2] During the refinement, all hydrogen atoms on water molecules and protonation were directly included in the molecular formula. The restraint command 'isor' was employed to restrain the oxygen atoms so as to avoid the ADP and NPD problems on them. This command leds to a final restraint value of 36. The crystal data and structure refinement are summarized in Table S1. CSD reference number 425204 contains the supplementary crystallographic data for this paper. This data may be obtained from the Fachinformationszentrum Karlsruhe, 76344 Eggenstein-Leopoldshafen, Germany (fax: (+49)7247-808-666; e-mail: crysdata@fiz-karlsruhe.de).

S1. A.Tézé, G. Hervé, *Inorg. Synth.* 1990, **27**, 85.

S2. G. M. Sheldrick, *SHELXL97, Program for Crystal Structure Refinement*, University of Göttingen: Göttingen, Germany, 1997; G. M. Sheldrick, *SHELXS97, Program for Crystal Structure Solution*, University of Göttingen: Göttingen, Germany, 1997.

Table S1. Crystal Data and Structure Refinement for **1**.

	1
Empirical formula	$C_6H_{68}K_8Mn_{12}Na_{10}O_{112}Si_2W_{12}$
M / g mol^{-1}	5396.96
λ / Å	0.71073
T / K	293(2)
Crystal dimensions / mm	0.18 × 0.14 × 0.08
Crystal system	Monoclinic
Space group	*C*2/c
a / Å	20.797(4)
b / Å	22.982(5)
c / Å	24.860(5)
β / °	100.51(3)
V / Å^3	11683(4)
Z	4
D_c / Mg m^{-3}	3.068
μ / mm^{-1}	13.468
F(000)	9912
θ Range / °	2.99 –27.44
Data / restraints / parameters	13221 / 36 / 708
R_1 ($I > 2\sigma(I)$)[a]	0.0563
wR_2 (all data)[a]	0.1339
Goodness-of-fit on F^2	1.029

[a] $R_1 = \sum||F_0|-|F_C||/\sum|F_0|$; $wR_2 = \sum[w(F_0^2-F_C^2)^2]/\sum[w(F_0^2)^2]^{1/2}$

Table S2. Bond valence sum calculations of compound **1**.[S3,S4]

Compound **1**					
Bonds	Bond length (Å)	BVS	Bonds	Bond length (Å)	BVS
Mn(1)-O(19)	1.883(9)	0.715435	Mn(4)-O(14)	1.845(9)	0.777959
Mn(1)-O(18)	1.920(10)	0.648753	Mn(4)-O(20)	1.855(9)	0.757215
Mn(1)-O(14)	1.942(10)	0.611303	Mn(4)-O(26)	1.865(10)	0.738619
Mn(1)-O(26)	1.944(9)	0.606695	Mn(4)-O(32)	1.936(10)	0.609653
Mn(1)-O(10)	2.113(11)	0.385062	Mn(4)-O(39)	1.945(10)	0.595003
Mn(1)-O(30)	2.194(9)	0.308694	Mn(4)-O(34)	1.946(11)	0.593381
$V_{Mn(1)}$ = **3.28**			$V_{Mn(4)}$ = **4.07**		
Mn(2)-O(17)	1.878(10)	0.726738	Mn(5)-O(38)#4	2.134(10)	0.368775372
Mn(2)-O(27)	1.879(10)	0.724777	Mn(5)-O(19)#4	2.146(10)	0.357006961
Mn(2)-O(20)	1.939(10)	0.61628	Mn(5)-O(33)	2.188(9)	0.318008974
Mn(2)-O(26)	1.944(9)	0.606695	Mn(5)-O(16)	2.196(10)	0.311880513
Mn(2)-O(11)	2.154(10)	0.344681	Mn(5)-O(7)	2.212(10)	0.298681235
Mn(2)-O(30)	2.225(9)	0.283884	Mn(5)-O(29)#4	2.336(8)	0.213225411
$V_{Mn(2)}$ = **3.30**			$V_{Mn(5)}$ = **1.87**		
Mn(3)-O(38)	1.894(9)	0.694478	Mn(6)-O(5)	2.022(11)	0.499128405
Mn(3)-O(36)	1.932(9)	0.626694	Mn(6)-O(15)#4	2.037(11)	0.47929815
Mn(3)-O(20)	1.942(9)	0.609983	Mn(6)-O(16)#4	2.108(9)	0.39476704
Mn(3)-O(14)	1.989(10)	0.538381	Mn(6)-O(33)	2.112(9)	0.390522275
Mn(3)-O(8)	2.127(11)	0.370764	Mn(6)-O(29)#4	2.113(9)	0.389468234
Mn(3)-O(30)	2.184(9)	0.317151	Mn(6)-O(29)	2.157(9)	0.345800973
$V_{Mn(3)}$ = **3.16**			$V_{Mn(6)}$ = **2.50**		

S3. The valence sum calculations are performed on a program of bond valence calculator, version 2.00 February 1993, written by C. Hormillosa, with assistance from S. Healy, distributed by I. D. Brown.

S4 I. D. Brown, D. Altermatt, *Acta Crystallogr.*, 1985, **B41**, 244.

Section 2 Supplementary Structural Figures

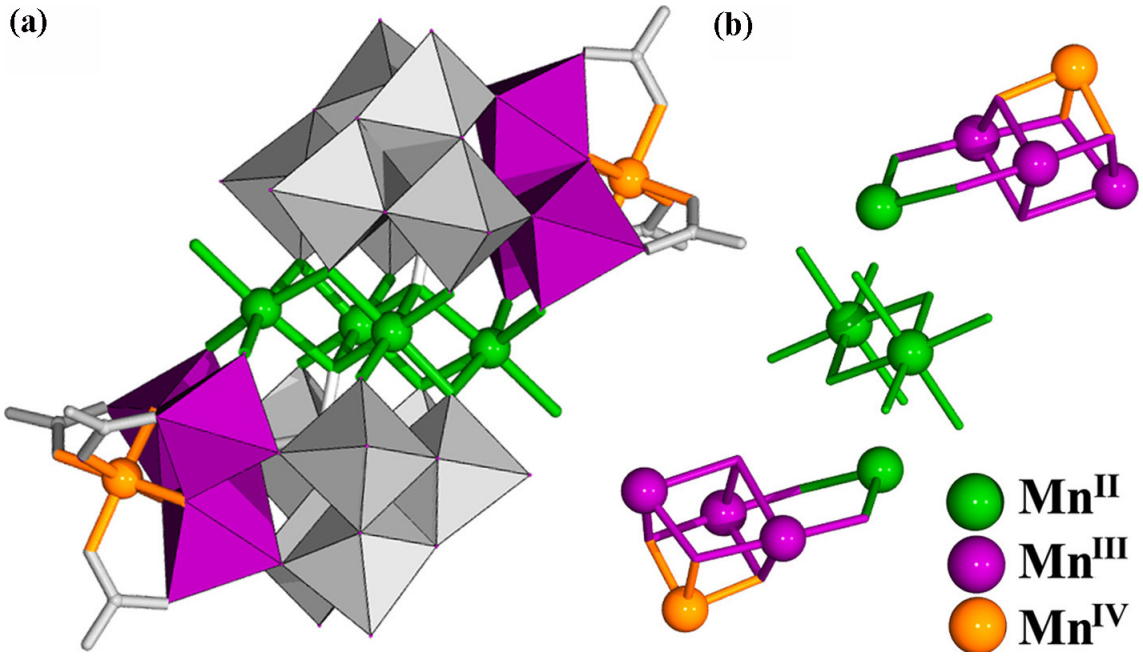

Fig. S1. (a) Combined ball-and-stick/polyhedral view of polyoxoanion **1**; (b) ball-and-stick view of the appended $\{Mn^{IV}Mn^{III}_3Mn^{II}\}$ cubanes and the $\{Mn_2\}$ linker in polyoxoanion **1**.

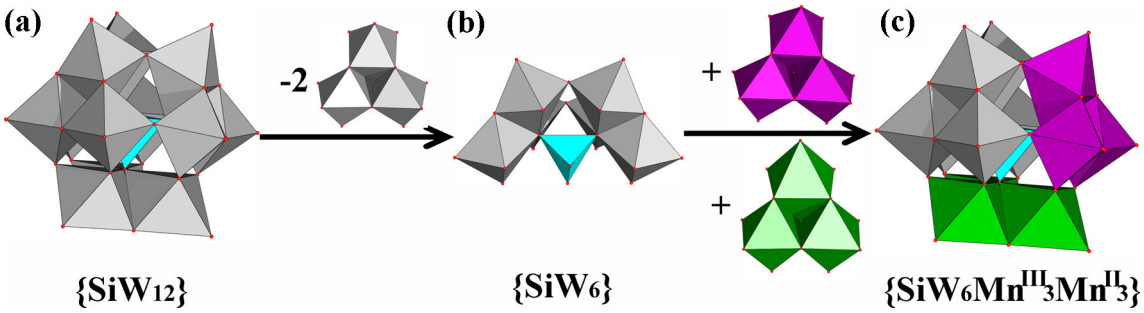

Fig. S2. Polyhedral view of $\{SiW_{12}\}$ (a), $\{\beta\text{-}SiW_6\}$ (b) and $\{SiW_6Mn^{III}_3Mn^{II}_3\}$ (c).

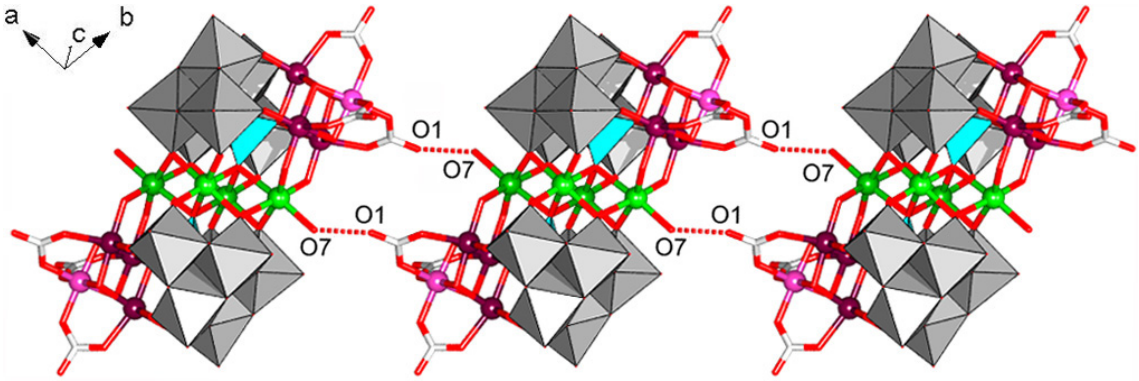

Fig. S3. Combined ball-and-stick/polyhedral view of the intermolecular interactions between the adjacent polyoxoanions.

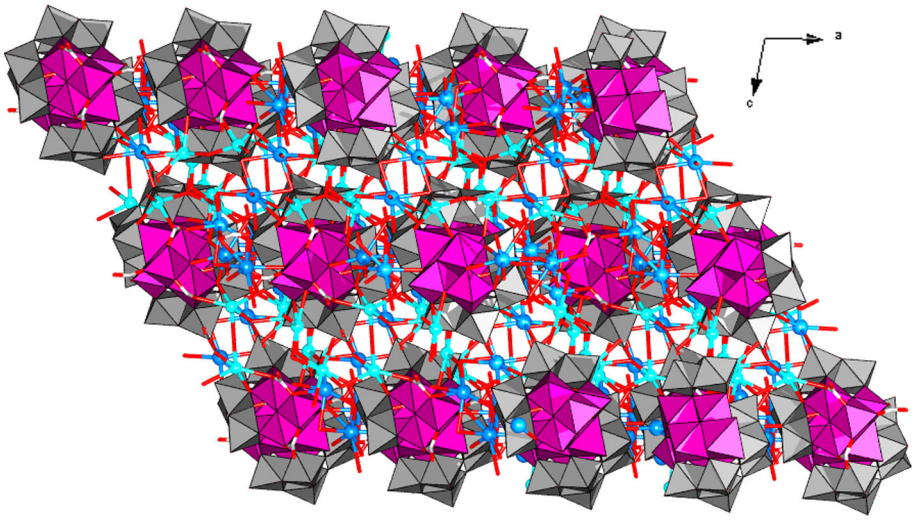

Fig. S4. View of the 3D packing of the structure for **1**.

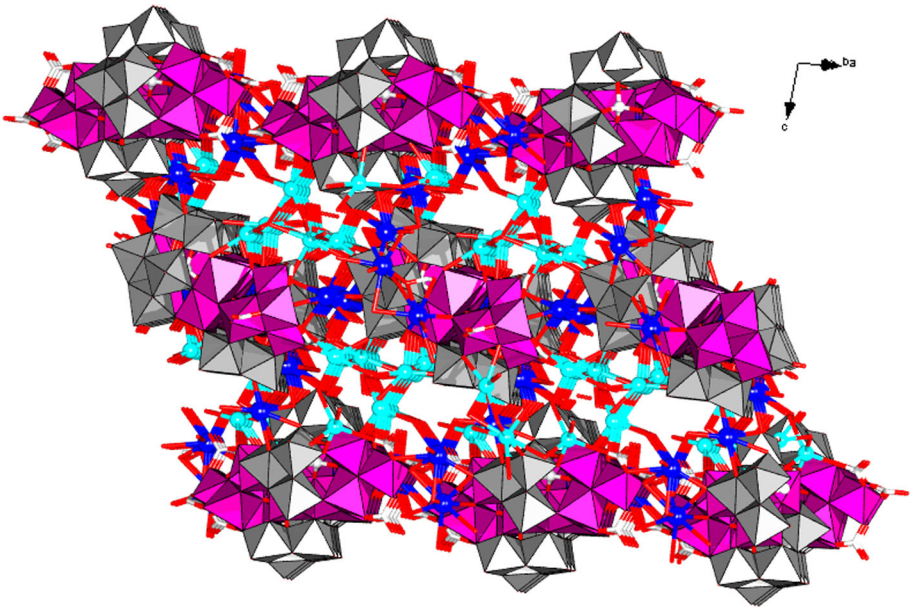

Fig. S5. View of the 3D packing of the structure for **1**.

Section 3 Supplementary Magnetic data

Magnetic Measurements

The dc magnetic susceptibility measurements of **1** were obtained with the use of a Quantum Design SQUID magnetometer MPMS-XL. This magnetometer works between 1.8 and 300 K for dc applied fields ranging from -7 to 7 T. Measurements of *M* versus *H* were performed at 100 K to check for the presence of ferromagnetic impurities, which were found to be systematically absent. Measurements of ac susceptibility were performed on a Quantum Design susceptometer PPMS, made with an oscillating ac field of 1 Oe and ac frequencies ranging from 10 to 10000 Hz without applied dc fields. Magnetic measurements were performed on a finely ground crystalline sample of 6.06 mg. The magnetic data were corrected for the sample holder and the diamagnetic contribution.

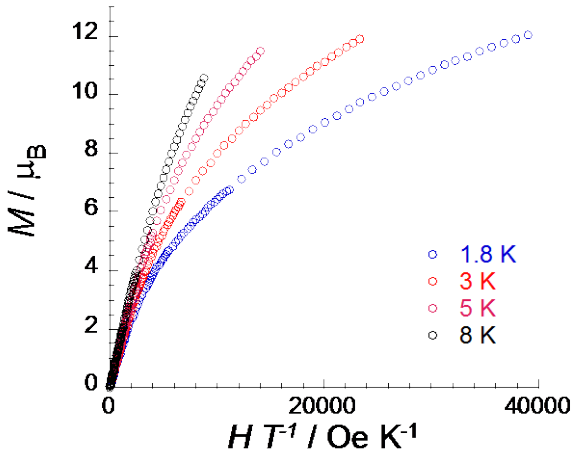

Fig. S6. Field dependence of the magnetization as *M* vs *H/T* plot for **1** between 1.8 and 8K with sweep-rates of 100 – 200 Oe/min. Indeed, a linear field dependence is observed above **1** T, suggesting the progressive-field-induced population of the low-lying states of the $\{Mn_{12}\}$ core in **1** (these states are also thermally populated above 1.8 K as seen on the χT vs *T* data) and also likely the presence of magnetic anisotropy induced by the anisotropic Mn^{III} metal ions (both phenomena are also seen by the non-superposition of the *M* vs *H/T* data as shown in Fig. S6).

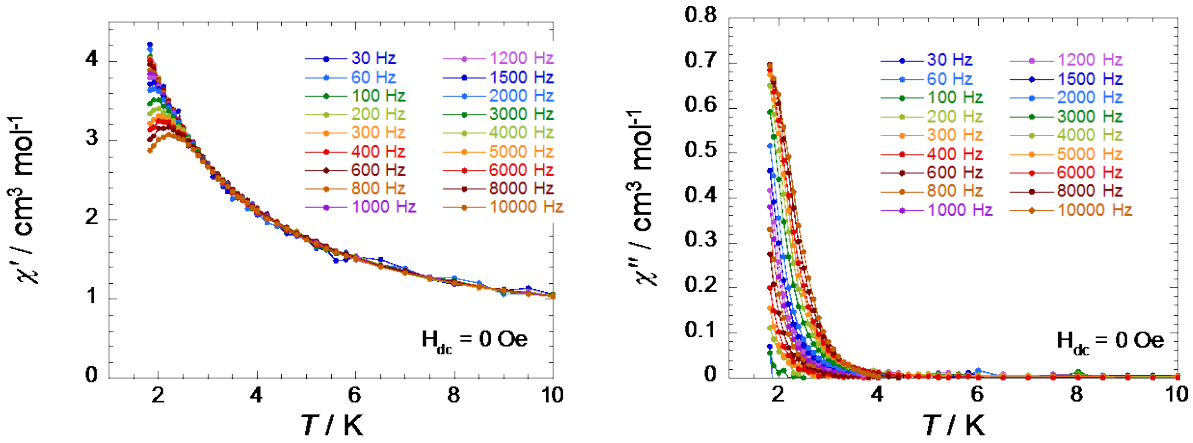

Fig. S7. Temperature dependence of the real (χ', left) and imaginary (χ'', right) parts of the *ac* susceptibility for a polycrystalline sample of **1** in zero-dc field at different ac frequency between 30 and 10000 Hz. Solid lines are guides.

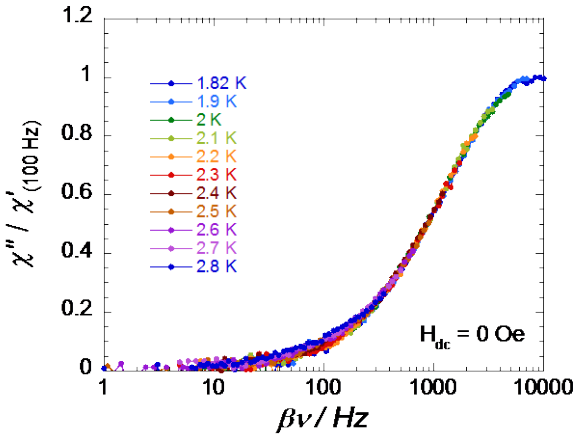

Fig. S8. Scaled frequency dependence of the out-of-phase component of the ac susceptibility normalized by the zero-frequency in-phase susceptibility (taken experimentally at 100 Hz) at different temperatures between 1.82 and 2.8 K (with H_{ac} = 1 Oe and H_{dc} = 0 Oe) for **1**. β is the scaling parameter equal to 1 for the data at 1.82 K.

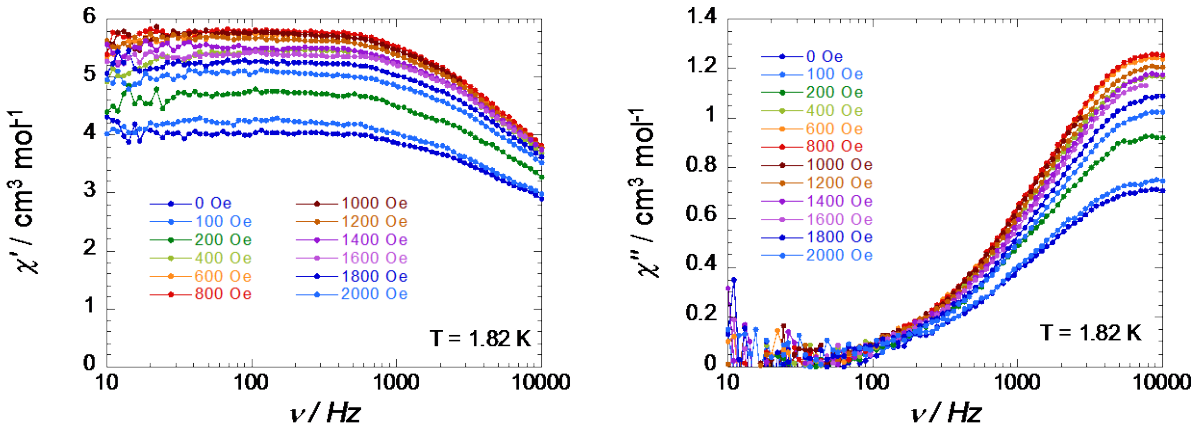

Fig. S9. Frequency dependence of the real (χ', left) and imaginary (χ'', right) parts of the *ac* susceptibility for a polycrystalline sample of **1** at 1.82 K at different *dc*-field between 0 and 2000 Oe. Solid lines are guides.

Section 4. Supplementary Physical Characterizations

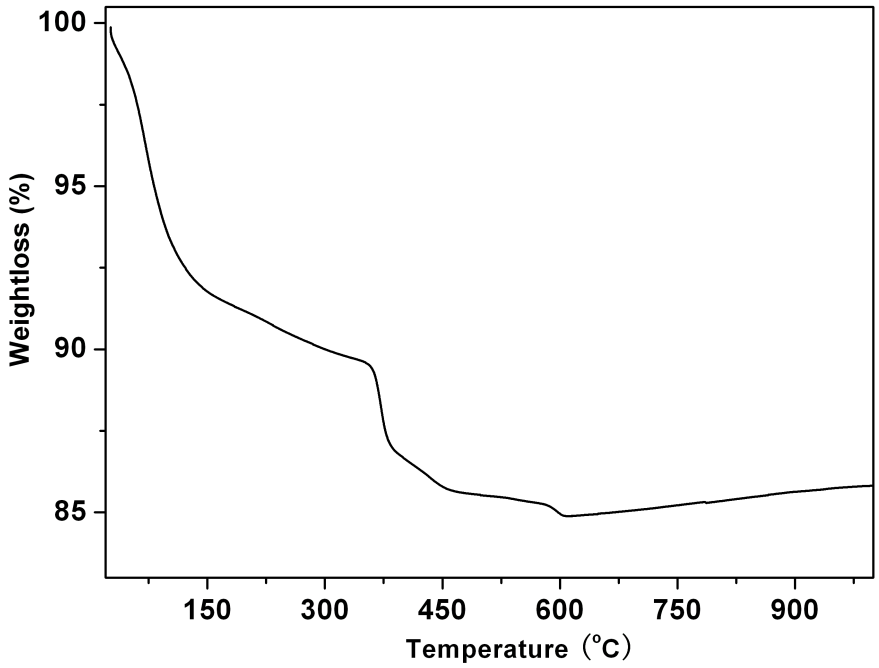

Fig. S10. The first weight loss of 10.53 % in the range of 24 ~ 358 °C are attributed to the loss of all lattice water molecules and coordinated water molecules (calcd. 10.67%); the second weight loss in the range of 358 ~ 610 °C corresponds to loss of the CO_3^{2-} ions.

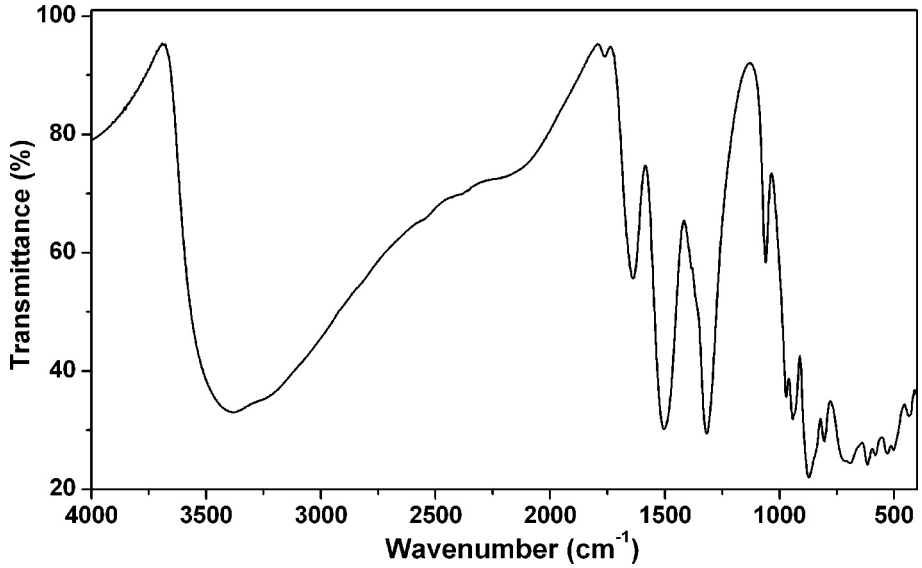

Fig. S11. IR spectrum for **1** at room temperature.